

Hydrogen-Bonded Layer-by-Layer Assembly
of Poly(Vinyl Alcohol) and Tannic Acid

by

Caitlin Sample

Submitted to the
Department of Materials Science and Engineering
in Partial Fulfillment of the Requirements for the Degree of

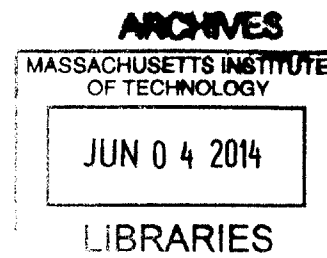
Bachelor of Science

at the

Massachusetts Institute of Technology

June 2014

©2014 Caitlin Sample
All rights reserved



The author hereby grants to MIT permission to reproduce and to
distribute publicly paper and electronic copies of this thesis document in whole or in part
in any medium now known or hereafter created.

Signature redacted

Signature of Author.....
Department of Materials Science and Engineering
May 2, 2014

Signature redacted

Certified by.....
Michael F. Rubner
TDK Professor of Polymer Materials Science and Engineering
Thesis Supervisor

Signature redacted

Accepted by.....
V V / Jeffrey C. Grossman
Carl Richard Soderberg Associate Professor of Power Engineering
Chairman, Undergraduate Committee

Hydrogen-Bonded Layer-by-Layer Assembly of Poly(Vinyl Alcohol) and Tannic Acid

by

Caitlin Sample

Submitted to the Department of Materials Science and Engineering
on May 2, 2014 in Partial Fulfillment of the
Requirements for the Degree of Bachelor of Science in
Materials Science and Engineering

ABSTRACT

Hydrogen-bonded multilayer thin films containing tannic acid (TA) and poly(vinyl alcohol) (PVA) were assembled under different pH conditions, and film growth and dissolution behavior was assessed through profilometry. Optimal film growth was achieved at pH 4.0, which contrasted with uncontrollable assembly at lower pH and lack of growth at higher pH. Changes in growth behavior due to variations in the molecular weight and degree of hydrolysis of PVA, as well as the concentration of the two components, were also investigated. High molecular weight PVA resulted in thicker films than low molecular weight PVA in two cases: fully hydrolyzed PVA at a concentration of 1.0 mg/mL and partially hydrolyzed PVA at a concentration of 0.1 mg/mL. In addition, the dynamic adsorption and desorption behavior of these films was investigated using QCM-D. The QCM-D results showed that each polymer immersion step involves both the deposition and removal of mass to and from the system, with the degree of removal determining the extent to which film assembly is successful. The pH stability of the PVA/TA films was higher than other previously investigated PVA based multilayer systems, which is consistent with the high pKa value of TA of 8.5. This increased pH stability, combined with the antioxidant, antimicrobial, antimutagenic, antitumor, and antibacterial properties of TA and the biocompatibility of PVA, makes the PVA/TA system attractive for biomedical applications, including drug delivery and sensing.

Thesis Supervisor: Michael F. Rubner

Title: TDK Professor of Polymer Materials Science and Engineering

Contents

1	Introduction and Theory	5
1.1	Layer-by-Layer Assembly	5
1.2	Poly(Vinyl Alcohol) and Tannic Acid	8
2	Materials and Methods	10
2.1	Materials	10
2.2	Methods	11
2.2.1	PGMA Surface Treatment	11
2.2.2	Layer-by-Layer Assembly	11
2.2.3	Profilometry	12
2.2.4	Dynamic Light Scattering	12
2.2.5	Quartz Crystal Microbalance with Dissipation Monitoring (QCM-D)	12
3	Results and Discussion	13
3.1	Effect of pH on Assembly	13
3.2	Effect of Concentration on Assembly	17
3.3	pH Stability	22
4	Conclusions and Outlook	23

List of Figures

1	Schematic of polymeric self-assembly in solution compared with the structure produced by LbL assembly.	5
2	Schematic of film dissolution.	7
3	Structure of fully and partially hydrolyzed poly(vinyl alcohol) (PVA) and tannic acid (TA).	9
4	Schematic of layer-by-layer assembly of PVA/TA.	12
5	Dry film thicknesses of $(PVA_F/TA)_{30}$ films assembled under different pH conditions. Photograph of mixtures of PVA_F and TA.	14
6	AFM topography images of $(PVA_F/TA)_{30}$ films assembled at (a) pH 2.0 and (b) pH 4.0.	15
7	Dry film thickness of PVA/TA assembled at different pH conditions with different degrees of hydrolysis and molecular weights of PVA.	16
8	Growth behavior of PVA/TA films assembled with different solution concentrations.	17
9	Hydrated mass evolution curves for PVA_F/TA at low and high concentrations.	19
10	Schematic of processes underlying film assembly of PVA_F and tannic acid.	19
11	Hydrated mass evolution curves for PVA_P/TA at low and high concentrations.	20
12	Schematic of processes underlying film assembly of PVA_P and tannic acid.	21
13	Growth behavior of PVPON/TA films assembled at pH 4.0 at low (0.1 mg/mL) and high (1.0 mg/mL) concentrations.	21
14	pH dissolution curve of $(PVA_F/TA)_{30}$ and $(PVA_P/TA)_{30}$ films assembled at pH 4.0 using high-molecular-weight PVA.	22
15	Schematic of selected applications of tannic acid-based multilayers.	24

1 Introduction and Theory

1.1 Layer-by-Layer Assembly

In the two decades since its development by Decher^{1;2}, layer-by-layer (LbL) assembly has proven successful as a relatively simple but effective way of fabricating multilayer thin films. The process of LbL assembly of polymeric multilayer films begins by exposing a substrate to a solution of polymer that forms a single conformal layer on the surface. After any excess polymer is rinsed off, this layer is then exposed to a second polymer solution that, if it is able to form interpolymer complexes with the first in solution, deposits a second layer. The excess of the second species is then rinsed, and the cycle begins again with exposure to the first polymer. This alternating exposure causes a series of bilayers to be built up, producing a periodic film with a well understood and easily controlled structure and thickness, such as that shown in Figure 1. Furthermore, varying the component molecules used allows mechanical, electronic, optical, and other properties to be tuned as well. The versatility of polymer pairings and the self-limiting nature of this process has encouraged extensive research using the LbL technique^{3;4}

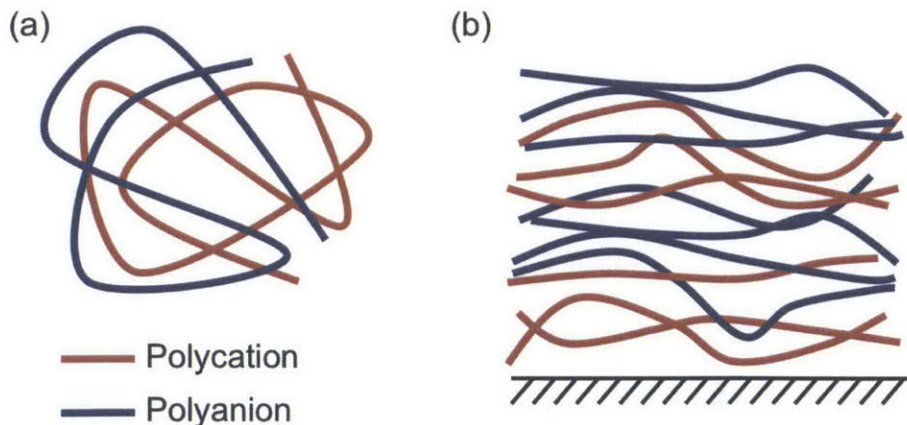


Figure 1: Schematic of (a) polymeric self-assembly in solution compared with (b) the structure produced by LbL assembly. The driving force in this case is electrostatic.

While much of the LbL field focuses on films assembled through electrostatic attraction, other driving

forces can be used to fabricate LbL multilayer systems, including hydrogen bonding. The ability of many pairs of polymers to form hydrogen-bonded complexes within solution has been known for decades^{5;6;7}, but assembling high quality films from these same polymer pairs had proven difficult. Shortly after the development of LbL assembly, Stockton and Rubner demonstrated that the technique could be extended to hydrogen-bonded systems by assembling polyaniline with a variety of other polymers, including poly(vinylpyrrolidone) (PVPON), poly(vinyl alcohol) (PVA), poly(acrylamide) (PAAm), and poly(ethylene oxide) (PEO), and sulfonated polystyrene (SPS)⁸.

Hydrogen-bonded LbL films differ from their electrostatic counterparts in a number of ways. One of the reasons that the assembly of electrostatic films is relatively well controlled is the charge compensation mechanisms that mediate the polymer deposition, and hydrogen-bonded films lack these mechanisms. As a result, hydrogen-bonded films tend to have a much larger bilayer thickness since polymers in these films tend to deposit in less tightly bound loops⁸. The thickness of these bilayers also depends on the number of intermolecular contacts and therefore on the strength of the interpolymer interaction, with more weakly interacting polymers resulting in thicker films⁹. A third factor that affects the bilayer thickness of weakly bound hydrogen-bonded films is the molecular weight of the component polymers, with a sevenfold increase in bilayer thickness measured when the molecular weight of PEO used to assemble poly(acrylic acid) (PAA)/PEO films was increased from 1.5 to 20 kDa¹⁰. The reason behind this effect is that, in weakly bound systems, a sufficient number of binding sites is necessary to cause polymer deposition, and this critical amount is difficult to reach with shorter polymers.

Another structural difference between hydrogen-bonded and electrostatic films arises from the ability of polymers to diffuse through the film. In the electrostatic case, there is some interpenetration between polymer layers, but interactions typically only occur on the scale of a bilayer or two. In hydrogen-bonded films, however, polymers are often able to diffuse to substantial depths within the film. Neutron reflectivity experiments revealed the extent of this diffusion, which takes place to varying degrees depending on the

strength of the intermolecular forces, with weakly bound systems showing greater amounts of diffusion than strongly bound films⁹. For example, the weakly interacting pair of PEO and poly(methacrylic acid) (PMAA) were found to be completely interdiffused, with no discretely layered structure remaining.

One of the largest differences between hydrogen-bonded films and their electrostatic counterparts is in the pH responsiveness of hydrogen-bonded systems. The nature of hydrogen-bonding interactions means that as the pH of the environment increases, the bonds that hold these films together gradually weaken and break as the hydrogen-bond donor molecules become deprotonated. The breaking of the bonds within these films leads first to film swelling, as the layers are held more tenuously together, and finally, if pH conditions are elevated beyond the critical pH (pH_{crit}) of the film, the film may dissolve, as shown in Figure 2. The exact value of the pH_{crit} depends on a number of factors, including the strength of the interaction between the two polymers and the pK_a of the hydrogen-bonding donor. This allows the dissolution profile of the film to be tuned to a desired pH.

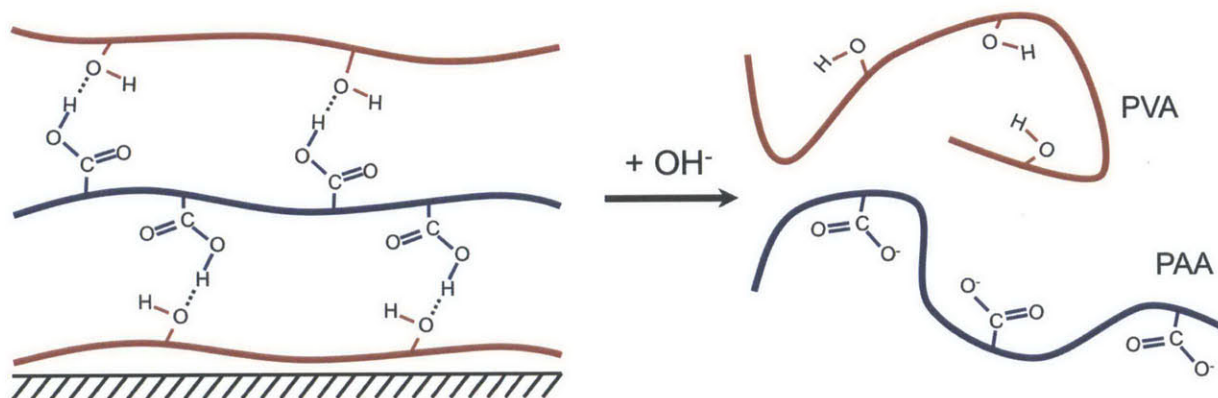


Figure 2: Schematic of the dissolution of a hydrogen-bonded film composed of poly(vinyl alcohol) (PVA) and poly(acrylic acid) (PAA) occurring as a result of an increase in environmental pH.

Additionally, the pH conditions under which the films are assembled have been shown to have an effect on the resulting film. Just as assembled films will dissolve as the environment becomes more basic, film assembly is hindered and even prevented entirely if the assembly pH is raised to values near the pH_{crit} . If the hydrogen-bond donor is deprotonated, no interactions can occur between the two polymers, and no film

will be deposited. Conversely, decreasing the pH substantially may also have adverse effects on the film assembly. For instance, PAA/PVPON multilayers assembled at low pH values were shown to be rough and unusually thick due to PAA becoming increasingly uncharged and collapsing on itself hydrophobically. As a result, insoluble clumps of PAA were deposited instead of flexible polymer chains¹³.

Due to their varied properties, hydrogen-bonded LbL films are attractive for a variety of applications. Their pH-triggered dissolution, coupled with their ability to absorb large quantities of biofunctional molecules such as dyes or drugs makes them appealing for molecular delivery. Most hydrogen-bonded films are also readily cross-linked chemically or thermally, allowing them to form hydrogels that are stable at physiological conditions for biomedical applications. Depending on the degree of hydrolysis, some pH responsiveness can also be maintained to give reversible, pH-triggered swelling. Additionally, hydrogen-bonded systems allow for the incorporation of neutral polymers with low glass transition temperatures, allowing for the possibility of free-standing films and membranes for electrochemical devices, fuel cells, and a number of other applications. This tunability and diverse number of properties have opened up a variety of opportunities for hydrogen-bonded films, and the library of these systems is ever growing^{11;12}.

1.2 Poly(Vinyl Alcohol) and Tannic Acid

One polymer that is well suited for hydrogen-bonded films is poly(vinyl alcohol) (PVA), which is shown in both its fully hydrolyzed and partially hydrolyzed forms in Figure 3a. PVA is an easily chemically functionalizable molecule known for its biocompatibility and hydrophilicity, and the abundance of alcohol groups makes it an excellent hydrogen-bonding acceptor. As such, it has been paired with a variety of hydrogen-bonding partners using the LbL technique, including polyaniline⁸, clay particles^{14;15}, poly(acrylic acid) (PAA), and poly(methacrylic acid) (PMAA)¹⁶. By varying the hydrogen bonding partner, films with a wide range of pH_{crit} values can be produced. In fact, Lee *et al.* found that, in addition to the hydrogen bonding donor, the degree of hydrolysis of PVA also affected the assembly characteristics and stability of

their films. PAA was only able to assemble with partially hydrolyzed PVA, while PMAA formed a more stable film with partially hydrolyzed PVA than fully hydrolyzed PVA due to the increased strength of the interaction¹⁶. This additional degree of freedom provides PVA systems with increased versatility in their design.

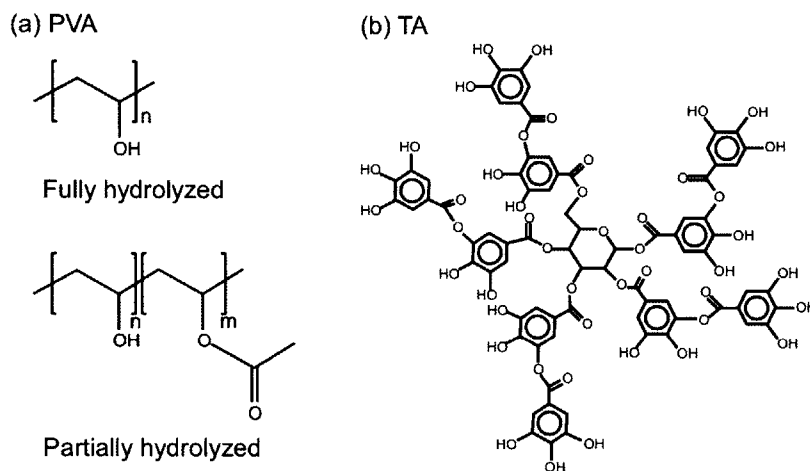


Figure 3: Structure of (a) fully and partially hydrolyzed poly(vinyl alcohol) (PVA) and (b) tannic acid (TA).

In this work, PVA is paired with tannic acid, which has been increasingly investigated as a component of multilayer films due to its variety of bioactive properties, including antitumor, antienzymatic, antibacterial, antimutagenic, and antioxidant activities¹⁷. Tannic acid is a polyphenolic molecule consisting of five digallic acid units attached to a glucose core, and its high abundance of hydroxyl groups makes it appealing for inclusion in hydrogen-bonded films. In fact, tannic acid has the maximum amount of hydroxyl groups of any tannin derivative¹⁸. Due to its high density of hydrogen-bonding donors and relatively high pK_a value of 8.5¹⁹, the inclusion of tannic acid in hydrogen-bonded multilayers tends to lead to more stable systems than those fabricated from most other polymers¹⁸.

For these reasons, tannic acid has been assembled with a variety of neutral polymers, including PVPON, PEO, PVCL, and PNIPAM^{19;20}, and due to its ability to remain protonated at basic pH values, assembly was able to be performed at pH 7.5. This allows for film deposition at physiological pH conditions, making

tannic-acid-based films attractive for biomedical applications. However, the LbL assembly of tannic acid in hydrogen-bonded films has not always led to the smooth, conformal coatings desired. For example, Zhou *et al.* noticed that the strong hydrogen bonding between PVPON and TA caused the formation of intermolecular complexes at low temperatures, leading to rough morphologies and different growth rates²¹. In this work, we sought to better understand how film assembly with small organic molecules differs from that of polymers by investigating the effect of a variety of assembly conditions, including pH, degree of hydrolysis of PVA, and concentration, on the growth behavior, morphology, and stability of hydrogen-bonded PVA/TA multilayer films.

2 Materials and Methods

2.1 Materials

Partially hydrolyzed poly(vinyl alcohol) (PVA_P, low molecular weight: $M_W = 24\,500$ g/mol, PDI = 1.99, 87-89% hydrolyzed, Sigma-Aldrich; high molecular weight: $M_W = 131\,000$ g/mol, PDI = 1.50, 87-89% hydrolyzed, Sigma-Aldrich), fully hydrolyzed poly(vinyl alcohol) (PVA_F, low molecular weight: $M_W = 21\,400$ g/mol, PDI = 1.22, 98-99% hydrolyzed, Sigma-Aldrich; high molecular weight: $M_W = 144\,000$ g/mol, PDI = 1.34, 98-99% hydrolyzed, Sigma-Aldrich), tannic acid (TA, $M_W = 1701$ g/mol, Sigma-Aldrich), poly(diallyldimethylammonium chloride) (PDAC, $M_W = 200\,000$ - $350\,000$ g/mol, 20% aqueous solution, Sigma-Aldrich), poly(sodium 4-styrene-sulfonate) (SPS, $M_W = 70\,000$ g/mol, Sigma-Aldrich), poly(vinyl pyrrolidone) (PVPON, $M_W = 360\,000$ g/mol, Sigma-Aldrich), 2-butanone (MEK, 99+% A.C.S. reagent, Sigma-Aldrich), poly(glycidyl methacrylate) (PGMA, $M_W = 25\,000$ g/mol, 10% solution in MEK, Polysciences) were used as received. Standard soda lime glass microscope slides and phosphate buffer saline (PBS) were obtained from VWR. Deionized water (DI, 18.2 M Ω -cm, MilliQ) was used in all aqueous polymer solutions and rinsing procedures.

2.2 Methods

2.2.1 PGMA Surface Treatment

The glass slides were first degreased by sonication in a 4% (v/v) solution of Micro-90 (International Products Co.) for 15 minutes, followed by two more 15-minute rounds of sonication in DI water. The slides were then dried with compressed air and treated with oxygen plasma (PDC-32G, Harrick Scientific Products, Inc.) for 2 minutes at 150 mTorr. After plasma treatment, the slides were immediately immersed for 20 seconds in a 0.1% (w/v) PGMA/MEK solution. Then, the PGMA-coated slides were placed in an oven at 110 °C for 30 minutes to produce covalent bonds between the PGMA and the plasma-treated glass surface. The slides were then allowed to cool to room temperature before being immersed in an aqueous solution of PVA (with the same concentration and pH as the assembly conditions of the film) for 30 minutes. After drying at ambient conditions, the slides were then returned to the oven for another 30 minutes at 110 °C to cross-link the epoxy groups in PGMA with the hydroxyl groups in PVA.

2.2.2 Layer-by-Layer Assembly

A schematic of the layer-by-layer (LbL) assembly of PVA/TA films is shown in Figure 4. Films were fabricated using a Stratosquence VI spin dipper (Nanostrata Inc.), the operation of which was controlled and monitored using StratoSmart v6.2 software. The LbL assembly of these films consisted of a 10-minute immersion step in the polymer solution followed by three rinsing steps of 2 minutes, 1 minute, and 1 minute. The pH of all solutions was adjusted to the desired value using 0.1 M HCl or 0.1 M NaCl as needed. No extra salt was used except for the polymers used in adhesion layers, to which solutions of 100 mM NaCl was added. The nomenclature for LbL films follows the convention of either (polycation/polyanion)_Z for electrostatically bound films or (hydrogen-bonding acceptor/donor)_Z for hydrogen-bonding-based films, with Z being the number of bilayers assembled.

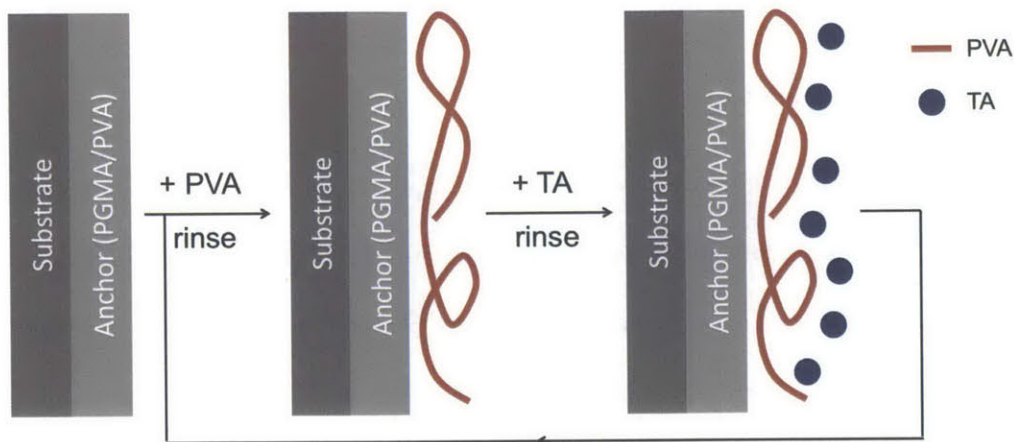


Figure 4: Schematic of layer-by-layer assembly of a single bilayer of a PVA/TA films. The PVA- and TA-immersion steps are repeated as many times as necessary to achieve the desired number of bilayers.

2.2.3 Profilometry

Dry film thicknesses were measured by removing a portion of the film with a razor and using a Tencor P16 surface profilometer to measure the difference in height between the film and the glass substrate. A $2\ \mu\text{m}$ stylus tip was used with a 2 mg force and a scanning rate of $50\ \mu\text{m/s}$. Linear scans of 1 mm were also taken on the film surface, and the resulting profiles were used to determine the R_a and R_q roughness values. Profilometry was also used in the pH-dissolution tests to determine the portion of film remaining on the surface by measuring the film thickness before and after 2 hours of immersion in DI water of specified pH conditions.

2.2.4 Dynamic Light Scattering

Dynamic light scattering (DLS) experiments were performed to determine the effective diameter of tannic acid in solution using ZetaPALS (Brookhaven Instruments Corp.).

2.2.5 Quartz Crystal Microbalance with Dissipation Monitoring (QCM-D)

Silica-coated QCM sensors (Q-Sense Inc.) were cleaned by 10 minutes of UV/ozone treatment followed by 30 minutes of immersion in 2% (v/v) sodium dodecyl sulfate (SDS) at room temperature. The sensors

were then rinsed with DI water and dried with compressed air. After a second UV/ozone treatment for 10 minutes, the baseline frequency and dissipation were recorded with a blank sensor exposed to pH 4.0 DI water, and these baselines were used to calibrate subsequent measurements. Film assembly then proceeded by flowing polymer and rinse solutions over the sensors at a flow rate of 150 $\mu\text{L}/\text{s}$. First, an adhesion layer of 3.5 bilayers of PDAC and SPS was assembled to substitute for the PGMA surface treatment. Then, TA and PVA were alternatively flowed over the surface for 5 minutes, with each immersion step followed by a 2 minute rinse step using pH 4.0 DI water. Finally, the Voigt viscoelastic model in the Q-Sense analysis software (Q-tools) was used to determine the hydrated mass evolution from the measured frequency and dissipation.

3 Results and Discussion

3.1 Effect of pH on Assembly

To determine the effect of the assembly pH on the growth of the PVA/TA films, the dry film thicknesses of 30-bilayer films assembled with fully hydrolyzed PVA at a variety of pH conditions were measured, as shown in Figure 5a. The films assembled thickest at low pH values due to tannic acid being fully protonated and therefore having the full amount of hydrogen-bonding donor sites available, with the greatest thickness of 2649 ± 1088 nm at pH 2.0. As the pH increases, tannic acid becomes increasingly deprotonated. This deprotonation weakens the hydrogen-bonding interactions, leading to increasingly thinner films at pH 3.0 and 4.0 and little to no film assembly at pH 5.0 and above. Although the pKa of tannic acid is 8.5 and therefore the tannic acid molecules are not fully deprotonated, the binding site density has become low enough that film assembly is no longer preferable.

These findings were further corroborated by mixing equal concentrations of the two components, as shown in Figure 5b. Both the PVA and tannic acid solutions were clear when unmixed in every case except for tannic

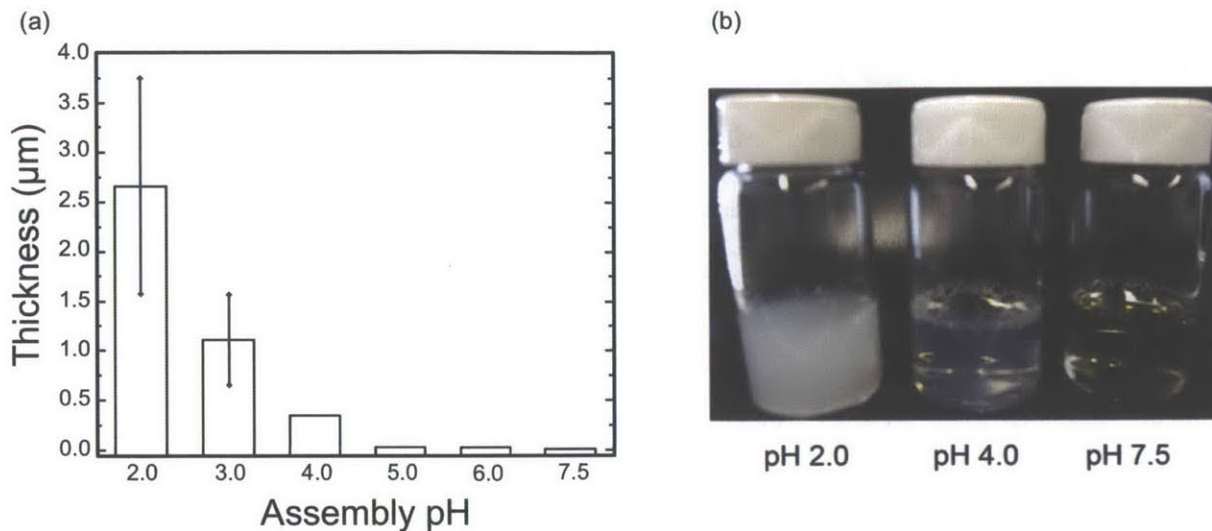


Figure 5: (a) Dry film thicknesses of $(\text{PVA}_F/\text{TA})_{30}$ films assembled under different pH conditions. The concentration of each component in solution was 1.0 mg/mL. The molecular weight of PVA used was 131-144 kDa. (b) Photograph of mixtures of PVA_F and TA. The concentration of each component in solution before mixing was 1 mg/mL.

acid at pH 7.5, in which case the solution had oxidized upon exposure to atmospheric oxygen and turned yellow in color. Upon mixing, the pH 2.0 solution showed a dramatic increase in turbidity, demonstrating the formation of complexes between PVA and tannic acid and therefore a significant enough driving force to bind the molecules together. As observed with the film assembly, this driving force decreases with increasing pH, with some turbidity apparent at pH 4.0 and none visible (and thus no complex formation) at pH 7.5.

Although the films assembled with the greatest thickness at pH 2.0, these films were relatively low quality. The standard deviation of 1088 nm is almost half of the average film thickness of 2649 nm, and this is due to the wide variability in film thicknesses observed. This variability shows the inconsistency and nonuniformity of the films produced. Furthermore, these films were not the smooth coatings desired but rather extremely rough, as apparent from the surface roughness values measured. The films assembled at pH 2.0 had R_a and R_q roughness values of 350 nm and 483 nm or around 13% and 18% of their thickness, respectively. This roughness stands in stark contrast to that of the pH 4.0 films, which had a thickness of 354 ± 5 nm and R_a and R_q values of 4.7 nm (1.3%) and 5.9 nm (1.7%), respectively. Atomic force microscopy (AFM) images

of the surface topography, as shown in Figure 6, are consistent with these measurements of the surface roughness. Figure 6a shows the surface of a film assembled at pH 2.0, which contains several features on the micron length-scale. In comparison, the surface of the film assembled at pH 4.0 is relatively smooth, with fewer apparent features, and those that are evident rarely exceed a few nanometers in size.

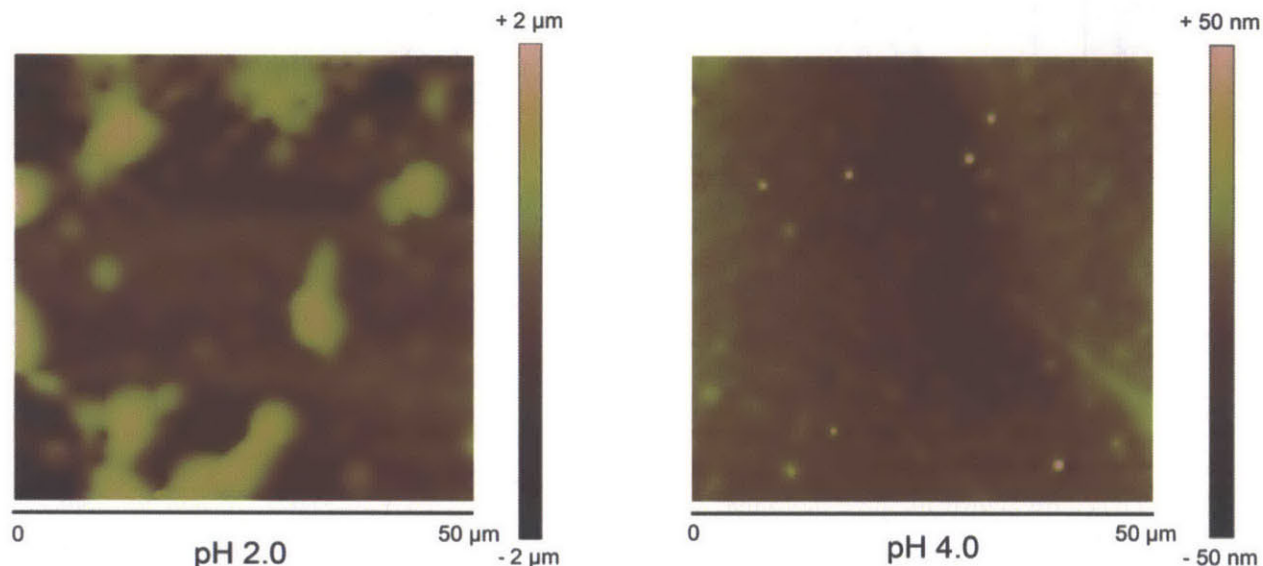


Figure 6: AFM topography images of $(\text{PVA}_F/\text{TA})_{30}$ films assembled at (a) pH 2.0 and (b) pH 4.0.

Many of the surface features observed through AFM have a particle- or clump-like nature to them, which resembles the behavior observed by Yang *et al.* with PAA at low pH values¹³ and suggests that the aggregation of tannic acid molecules at low pH values may be the source of increased surface roughness. As the pH decreases, tannic acid becomes less charged, which may increase hydrophobic interactions between tannic acid molecules. To test this hypothesis, dynamic light scattering (DLS) was used to assess the effective diameter of tannic acid in solution. For solutions of 1.0 mg/mL, the effective diameter was 47 ± 5 nm at pH 2.0 and 38 ± 5 nm at pH 4.0. The effective diameter at pH 2.0 is indeed larger, although only by a slim margin, suggesting that there is some preference for complex formation but that it cannot be the sole source of the increased roughness at low pH values.

In addition to the effect of assembly pH, the effects of degree of hydrolysis and molecular weight un-

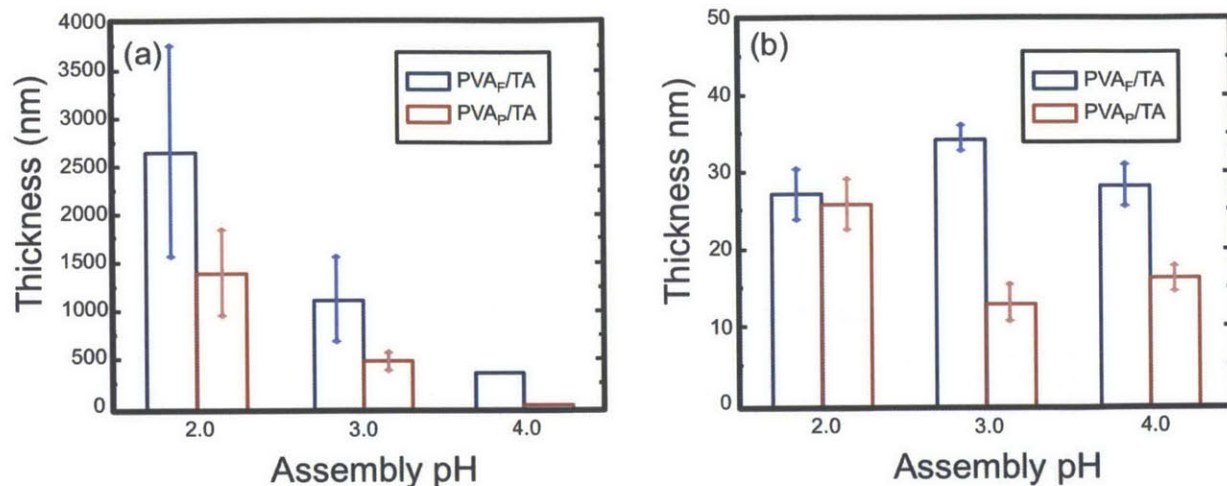


Figure 7: Dry film thicknesses of $(\text{PVA}_F/\text{TA})_{30}$ (blue bar) and $(\text{PVA}_P/\text{TA})_{30}$ (red bar) assembled at different pH conditions. The concentration of each component in solution was 1.0 mg/mL. The molecular weight of PVA used was (a) 131-144 kDa and (b) 21-25 kDa.

der different pH conditions were also investigated. The dry film thicknesses of both $(\text{PVA}_F/\text{TA})_{30}$ and $(\text{PVA}_P/\text{TA})_{30}$ are shown for high-molecular-weight (131-144 kDa) PVA in Figure 7a and low-molecular-weight (21-25 kDa) in Figure 7b. For high-molecular-weight PVA, a similar trend of decreasing thickness with increasing pH is observed for both the fully and partially hydrolyzed species and follows, as before, from the hydrogen-bonding nature of the intermolecular interactions. The primary difference between the two is that partially hydrolyzed PVA produced films approximately half as thick as those produced using fully hydrolyzed PVA at pH 2.0 and 3.0, and PVA_P films were even less thick relative to PVA_F films at pH 4.0. This difference, which arises due to the different content of acetate moieties between the two species, will be more thoroughly investigated and discussed in section 3.2.

In contrast with high-molecular-weight PVA, low-molecular-weight PVA barely assembled under any conditions. All films assembled with low-molecular-weight PVA exhibited a thickness of only a few dozen nanometers, which is extremely thin for a hydrogen-bonded system. As with the PAA/PEO systems fabricated by DeLongchamp and Hammond¹⁰, the weak nature of the hydrogen-bonding interactions within the film means that it is likely that longer molecules are needed to provide sufficient binding sites to allow for

stable films. Since tannic acid is inherently a small molecule, it is up to PVA to provide the long chains necessary for film assembly, and low-molecular-weight PVA is not of sufficient length.

3.2 Effect of Concentration on Assembly

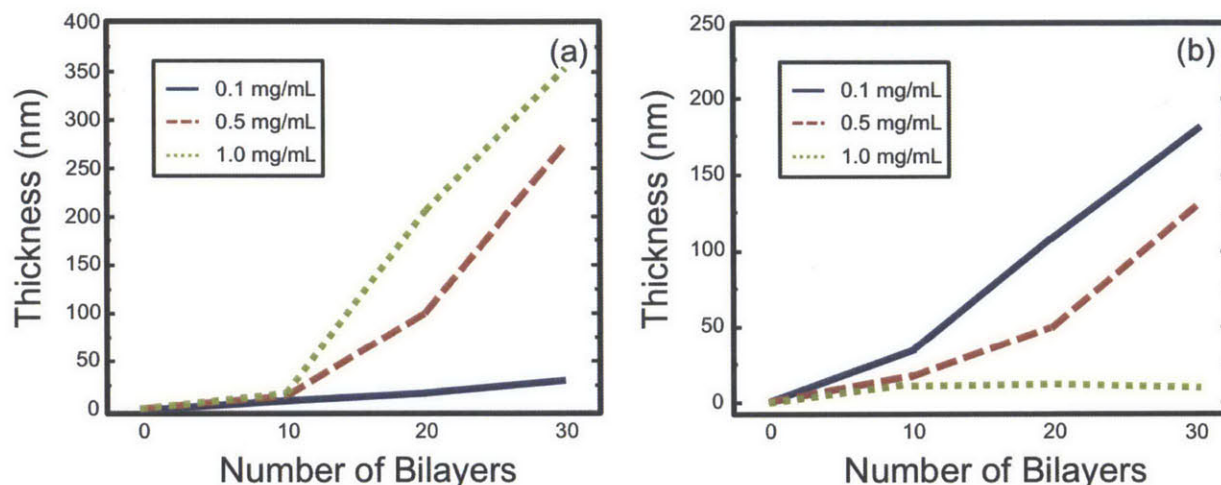


Figure 8: Growth behavior of (a) PVA_F/TA films and (b) PVA_P/TA films assembled at pH 4.0 with different solution concentrations: 0.1 mg/mL (solid blue line), 0.5 mg/mL (dashed red line), and 1.0 mg/mL (dotted green line).

The effect of concentration of the assembly solutions on the growth behavior of PVA/TA films was also investigated, and the dry film thicknesses of films assembled from solutions of concentrations 0.1 mg/mL, 0.5 mg/mL, and 1.0 mg/mL are shown in Figure 8. Some effect of concentration is expected within Lbl films, as at higher concentrations, polymer chains will deposit in a more crowded fashion and prevent each other from spreading out on the surface. Therefore, bilayer thickness should increase with concentration, which was observed for fully hydrolyzed PVA.

Additionally, a second contribution to the effect of concentration is the aggregation of tannic acid within solution, with aggregation becoming more preferable as the concentration of tannic acid increases. DLS was again performed to determine the effective diameter of tannic acid in solution, and in this case, the difference was substantially more dramatic. At pH 4.0, the effective diameter was 14 ± 5 nm for 0.1 mg/mL and 38 ± 5

nm for 1.0 mg/mL. Between these two concentrations there is a more than twofold increase in the effective diameter of tannic acid, showing that there is indeed increased aggregation at higher concentrations, which should also lead to a larger bilayer thickness at higher concentrations.

However, while both the crowding of polymer chains and aggregation of tannic acid molecules explain the trend in increasing bilayer thickness for fully hydrolyzed PVA, there is also a complex dependence on PVA's degree of hydrolysis. Partially hydrolyzed PVA exhibits the opposite trend from fully hydrolyzed PVA, with the lowest concentration of 0.1 mg/mL assembling with the greatest thickness. This trend is unexpected and cannot be explained by the factors considered so far.

To better understand this unusual growth behavior, quartz-crystal microbalance (QCM-D) measurements were taken of both the fully and partially hydrolyzed systems at low (0.1 mg/mL) and high (1.0 mg/mL) concentrations. QCM-D measures real-time changes in frequency and dissipation as material is deposited on the sensor's surface, allowing for visualization of the hydrated mass evolution at each step of the assembly. Figure 9 shows the hydrated mass curves for fully hydrolyzed PVA at low and high concentrations. These curves exhibit similar overall growth behavior to the film thickness measurements, with the high concentration film assembling more rapidly than the low concentration film. Furthermore, both curves are unusual shapes for the QCM-D profiles of LbL films. Most films tend to grow either linearly with each polymer step or increase in mass on one step and decrease in mass on the other. In these curves, the addition of mass from an immersion step is subsequently followed by partial removal of mass as molecules are lost to solution, leading to a relatively jagged shape.

By combining the DLS and QCM-D results, an idea of the processes underlying the film assembly begins to emerge. Previous studies have demonstrated that fully hydrolyzed PVA tends to form weaker hydrogen-bonded systems than its partially hydrolyzed counterpart due to the lack of acetate moieties to disrupt PVA's preference towards interacting with itself. Additionally, the acetate moieties increase the hydrophobic interactions with tannic acid, so their absence results in a more weakly interacting system. Therefore, fully

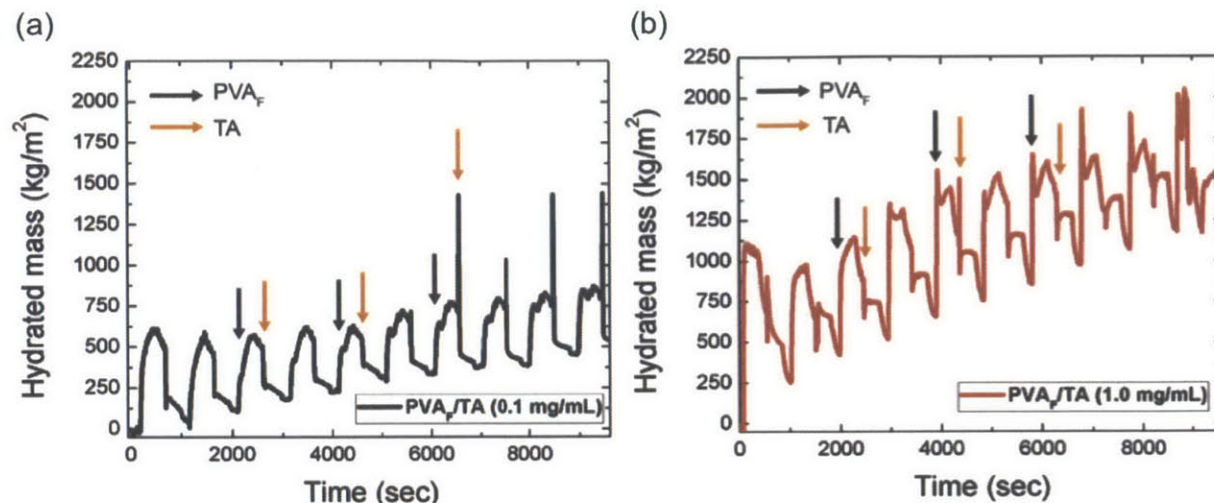


Figure 9: Hydrated mass evolution curves for PVA_F/TA at (a) 0.1 mg/mL and (b) 1.0 mg/mL showing locations of selected PVA immersion steps (black arrow) and TA immersion steps (orange arrow). Assembly took place at pH 4.0.

hydrolyzed PVA tends to assemble poorly at low concentrations. However, the QCM-D curve for the high concentration shows a larger increase in mass with less subsequent decrease in the PVA immersion step, showing that the polymer is better maintained on the surface. This is likely due to the increased amount of tannic acid aggregates on the surface, which provide enough of the necessary binding sites to bind PVA to the film. A schematic of these processes is shown in Figure 10.

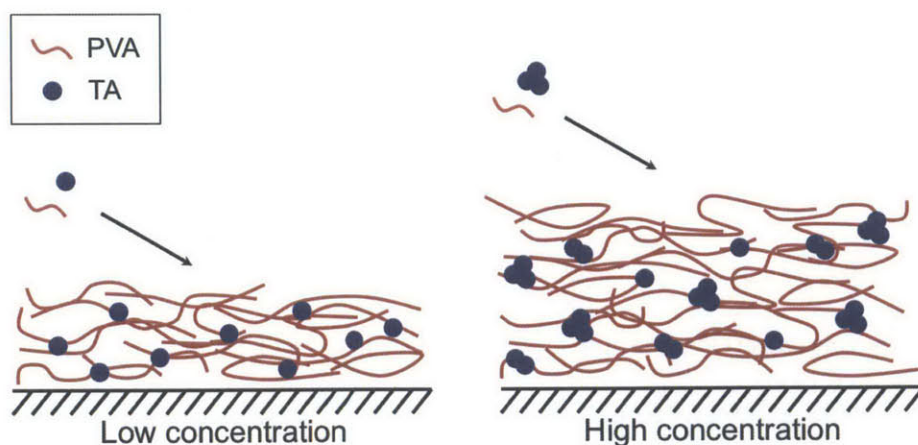


Figure 10: Schematic of processes underlying film assembly of PVA_F and tannic acid.

The hydrated mass curves of partially hydrolyzed PVA at low and high concentrations are shown in Fig-

ure 11a. As before, the growth trends match those of the measured film thickness, with partially hydrolyzed PVA assembling better at low concentrations than at high. Also similarly to the fully hydrolyzed case, each immersion step leads to an initial increase in mass followed by a subsequent decrease. However, what is specific to the partially hydrolyzed case is the extent to which that increase and decrease occur at the high concentration. The addition of PVA leads to a very large peak in the curve, but this added mass is almost entirely removed immediately, and the tannic acid immersion step removes most of the mass that remains. This leads to the slow growth observed in both the film thickness and QCM-D measurements.

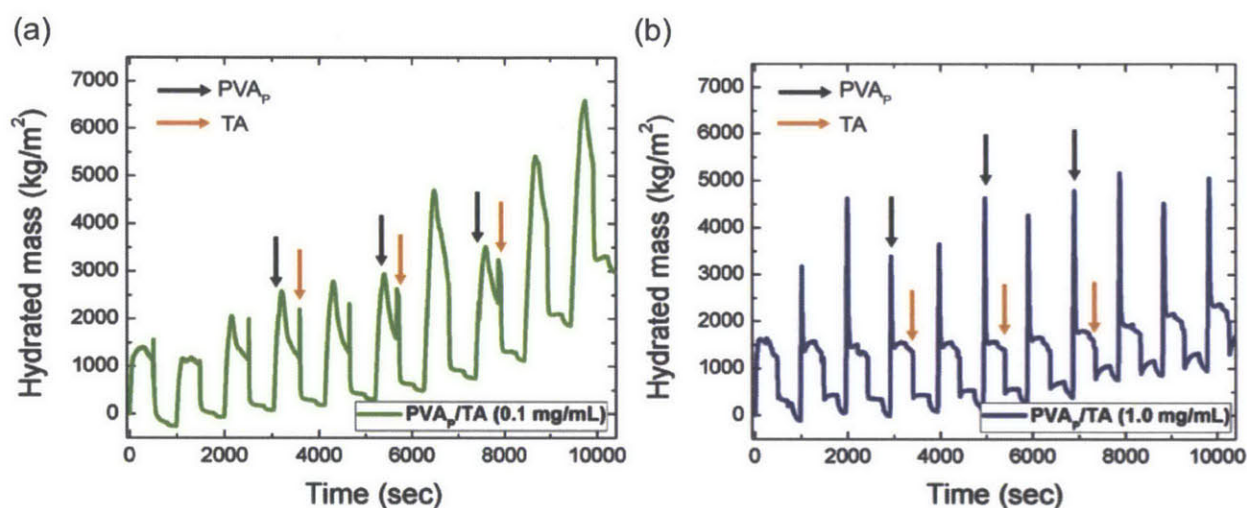


Figure 11: Hydrated mass evolution curves for PVA_P/TA at (a) 0.1 mg/mL and (b) 1.0 mg/mL showing locations of selected PVA immersion steps (black arrow) and TA immersion steps (orange arrow). Assembly took place at pH 4.0.

In the case of partially hydrolyzed PVA, the PVA-TA interactions are much stronger than those between PVA_F-TA. This allows the film to assemble well even at low concentrations. However, as tannic acid begins to aggregate at higher concentrations, this film growth is disrupted. The PVA immersion step leads to recently deposited tannic acid aggregates being pulled off of the film into solution to form PVA-TA complexes. The results is the lack of film assembly observed.

To determine the extent to which the effect of concentration really does depend on the aggregation of tannic acid and the strength of the PVA-TA interaction, films were also assembled from tannic acid

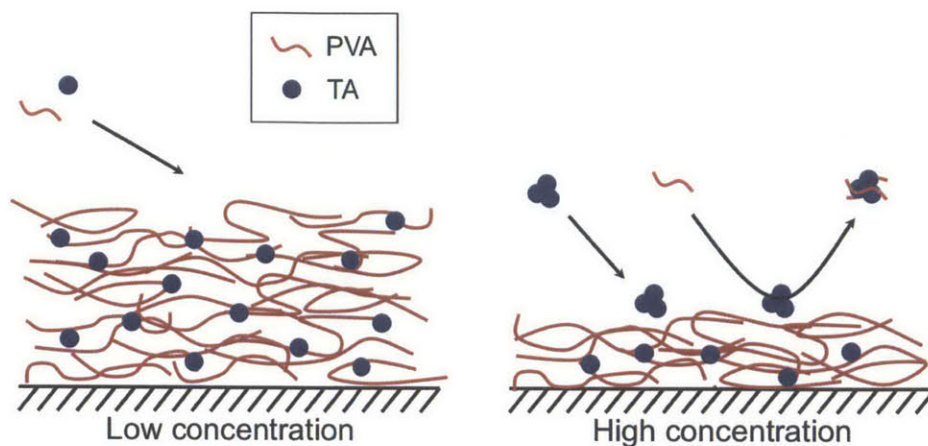


Figure 12: Schematic of processes underlying film assembly of PVA_P and tannic acid.

and poly(vinyl pyrrolidone) (PVPON), which forms strong hydrogen bonds. The dry film thicknesses of PVPON/TA films assembled at two different concentrations are shown in Figure 13. As expected from the PVA/TA experiments, the strongly interacting PVPON/TA assembles better at lower concentrations than at high. This is consistent with the hypothesis that at higher concentrations, the polymer, in this case PVPON, is solubilizing the tannic acid aggregates exposed on the film and reversing the previous deposition step.

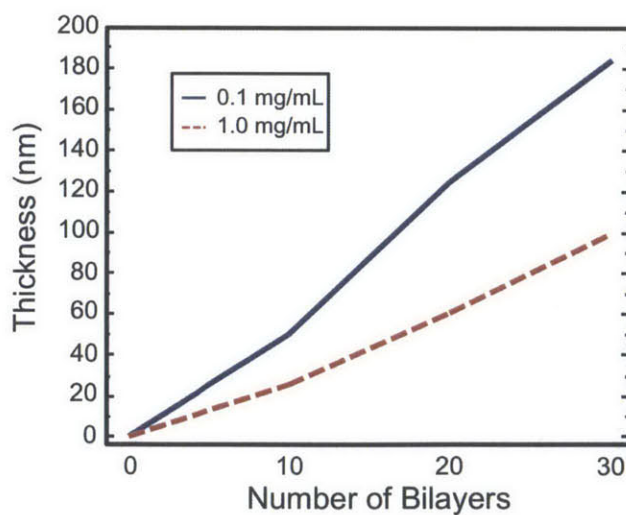


Figure 13: Growth behavior of PVPON/TA films assembled at pH 4.0 at low (0.1 mg/mL) and high (1.0 mg/mL) concentrations.

3.3 pH Stability

For the pH stability tests, $(\text{PVA}/\text{TA})_{30}$ films were assembled using high-molecular-weight PVA at pH 4.0 since these conditions produce the highest quality films. An intermediate concentration of 0.5 mg/mL was used to balance the contrasting trends of fully and partially hydrolyzed PVA. The dry film thicknesses of the resulting films were measured before and after exposure to various pH conditions, as shown in Figure 14. The critical pH (pH_{crit}) of PVA hydrogen bonded with weak polyacids has been measured previously and was found to range from 2.5 for PVA_P/PAA to 6.5 for PVA_P/PMAA . In contrast, both PVA_F/TA and PVA_P/TA exhibit higher pH_{crit} values of approximately 7.2 and 8.3, respectively. This is due to tannic acid's relatively high pK_a of around 8.5, allowing it to remain protonated to a higher pH value than the polyacids studied. As previously observed, partially hydrolyzed PVA interacts more strongly with tannic acid than fully hydrolyzed PVA, which results in its larger pH_{crit} . Additionally, both curves exhibit a sloping transition from fully intact to fully dissolved instead of the sharp dissolution observed in other systems. This is likely due to the small molecule nature of tannic acid, which may be loosely bound and diffuse from the film upon exposure to more basic conditions.

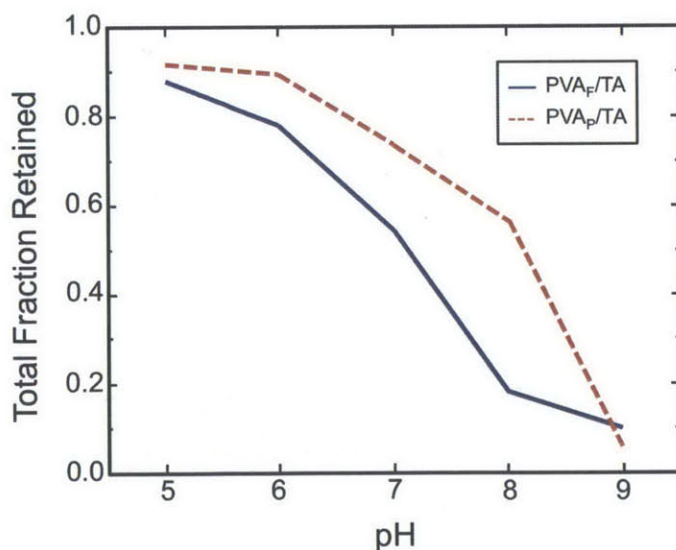


Figure 14: pH dissolution curve of $(\text{PVA}_F/\text{TA})_{30}$ and $(\text{PVA}_P/\text{TA})_{30}$ films assembled at pH 4.0 using high-molecular-weight PVA.

4 Conclusions and Outlook

In conclusion, it has been shown that multilayer films can be produced using hydrogen-bonding driven LbL assembly of poly(vinyl alcohol) and tannic acid. The growth behavior, morphologies, and pH stability of these films can be tuned by varying a number of variables, including assembly pH, molecular weight, degree of hydrolysis, and concentration. The highest quality, most reproducible films were produced by using high-molecular-weight PVA at a pH of 4.0. However, the effects of degree of hydrolysis and concentration are more complex, with fully hydrolyzed PVA assembling more thickly at high concentrations and partially hydrolyzed PVA assembling better at low concentrations. This behavior arises from a combination of the varying strength of the PVA/TA interaction due to the differing concentrations of acetate moieties and the increasing amount of tannic acid aggregation at higher concentrations in solution. These aggregates also form as a function of pH, with acidic conditions encouraging self-association of tannic acid due increased hydrophobic interactions. Therefore, by varying the concentration and pH, the amount of tannic acid aggregates within the film can be controlled.

In considering the potential uses for these films, it is important to understand the current applications of hydrogen-bonded LbL films containing tannic acid. Due to tannic acid's bioactive properties and the physiologically-relevant pH stability of tannic acid-based films, most work so far has been focused on biomedical applications. These include cell surface modification, targeted delivery of bioactive molecules, and sensing and detection, as shown in Figure 15.

In the first of these areas, cell surface modification, LbL films have proven particularly interesting due to their advantages over other techniques. The idea of cell surface engineering is to achieve some goal, such as providing additional protection to cells, without hindering cell function, which makes the tunable permeability of LbL films attractive^{22;23;24;25}. Additionally, LbL multilayers can be assembled on a variety of cell geometries with a well controlled thickness. However, polyelectrolyte multilayers have been unsuccessful due

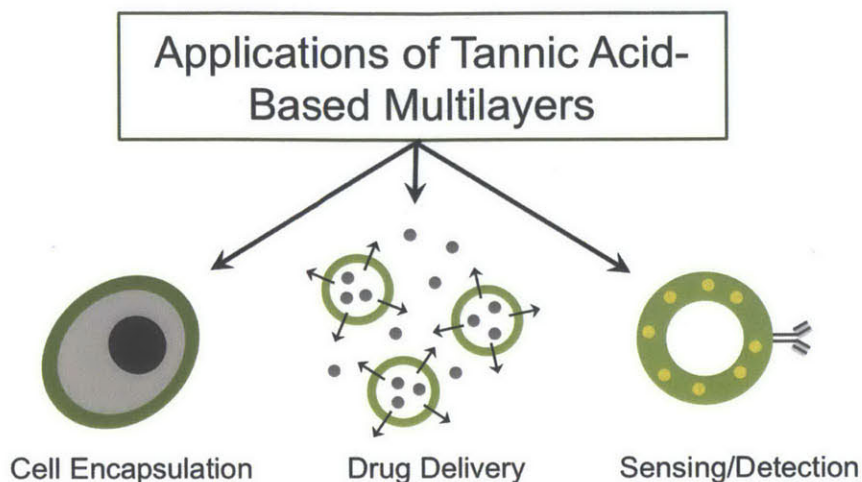


Figure 15: Schematic of selected applications of tannic acid-based multilayers, showing cell encapsulated in film, drugs (or other bioactive) molecules being released from multilayer microcapsules, and a multilayer capsule loaded with gold nanoparticles and functionalized with an antibody for targeted detection.

to the cytotoxicity of polycations^{26;27}. Therefore, interest has recently turned to hydrogen-bonded multilayers due to the ability to use neutral, biocompatible components.

Of specific interest to this study was the use by Kozlovskaya *et al.* of PVPON/TA multilayers for cell surface engineering. In addition to its high pKa, tannic acid was selected for its ability to hinder radical-induced oxidation, which allows for increased cell viability. Kozlovskaya *et al.* were able to successfully encapsulate *Saccharomyces cerevisiae* yeast cells in PVPON/TA shells. Not only did these coated cells shown high viability of almost 80%, they were substantially more viable than their counterparts coated with a standard polyelectrolyte multilayer composed of polyallylamine hydrochloride (PAH) and poly(styrene sulfonate) (PSS). Additionally, the PVPON/TA multilayers were almost five times as permeable as their polyelectrolyte analogues, allowing for improved exchange between the cells and their environment, which may account for the higher level of viability. Furthermore, coated cells maintained more of their function when coated with hydrogen-bonded films rather than polyelectrolyte films, and the hydrogen-bonded coating was shown to delay but not inhibit cell division.

However, although the PVPON/TA study shows the potential of tannic acid-based systems for cell

encapsulation, the PVA/TA multilayers produced in this work are unsuitable for this application due to the low pH necessary to fabricate them. Such a low pH would create a hostile environment, so these films cannot be deposited onto living cells. If the PVA-TA interaction could be further optimized to increase the pH window for assembly, though, such a film would likely prove useful for cell surface modification due to PVA's high degree of biocompatibility and ease of functionalization.

These properties of PVA, as well as the high pH stability of tannic acid, also make PVA/TA films an appealing candidate for the second application of tannic acid-based films, the targeted delivery of bioactive molecules such as drugs. One of the most common ways to use LbL films for molecule delivery is to produce microcapsules formed around or assembled with the molecule of interest. These microcapsules can then be functionalized with molecules such as antibodies to allow for selective targeting, and the molecule to be delivered is released from the capsule through increased film porosity^{29;30} or even film dissolution^{31;32}, which is made possible by the ability of hydrogen-bonded LbL films to respond to local pH or ionic conditions.

One of the first investigations of tannic acid's suitability as a LbL microcapsule component was carried out by Shutava *et al.*³³. They assembled polyelectrolyte multilayers by pairing tannic acid with one of two polycations, the strongly binding poly(dimethyldiallylamide) (PDDA) and the weakly binding PAH. When assembly was carried out on MnCO₃ microcores that were subsequently dissolved, hollow microcapsules were produced. The permeability of these capsules was shown to be pH-dependent, with a minimum around the assembly pH of 7, allowing for release molecules as pH conditions become increasingly acidic or basic. In particular, the physiological pH of 7.4 would allow for slow diffusion of molecules from the insides of the capsule outwards.

Capsules formed from hydrogen-bonded multilayers such as PVA/TA would have a number of advantages over these polyelectrolyte capsules. As mentioned previously, hydrogen-bonded films tend to be more biocompatible than their cytotoxic counterparts. Additionally, the pH-responsive nature of hydrogen-bonded films causes increased permeability and film dissolution with increasing pH instead of a minimum in the

center of the pH range. This allows for triggerable dissolution at a well understood pH value. While capsule composed of the most common tannic acid-based system of PVPON/TA were found to dissolve at the relatively high pH value of 10¹⁸, the critical pH values of PVA_F and PVA_P are closer to the physiological pH at 7.2 and 8.3, respectively. Due to the sloping nature of PVA/TA's pH dissolution profile, this means that PVA/TA experiences some loss of film integrity at physiological conditions without undergoing complete dissolution. The consequences for film permeability need to be investigated further, but it is likely that PVA/TA films are well tuned to allow triggerable molecular diffusion at the conditions within the body. Additionally, PVA's abundance of alcohol groups allows for covalent attachment of molecules, and Lee *et al.* demonstrating that PVA-based multilayer films could be successful functionalized post-assembly¹⁶. These free alcohol groups could be used to immobilize antibodies on the surface to allow for selective targeting by drug delivery capsules.

In addition to these applications, tannic acid-based films have also gained interest due to tannic acid's ability to interact with metal ions. In particular, tannic acid has been shown to strongly chelate^{34;35;36} and reduce metal ions^{37;38}. To take advantage of this property, Kozlovskaya *et al.* assembled PVPON/TA microcapsules and, after activating the tannic acid with borate buffers, exposed them to a solution containing gold ions. After exposure, TEM images revealed that the tannic acid within the films had successfully bound and reduced enough gold ions to produce gold nanoparticles of varying dispersities depending on the molecular weight of PVPON used.

The ability to grow gold nanoparticles within these microcapsules provides a method of producing composite organic-inorganic structures for biological applications due to the high biocompatibility of the components. Such nanoparticle production relies primarily on the presence of tannic acid, so the PVA/TA films fabricated in this work would be able to produce similar nanoparticles. Gold nanoparticles are often used for biochemical labeling due to their ability to be monitored *in situ*, and this, combined with the ability to conjugate various molecules such as antibodies and other proteins onto the free alcohol groups of PVA,

would make these composite PVA/TA-Au structures valuable for detection and sensing applications. These structures would also have tunable stability based both on the choice of PVA_F or PVA_P and the potential for cross-linking of PVA.

Hydrogen-bonded multilayer films composed of PVA and tannic acid have the potential for a variety of applications, especially in the biomedical field. Tannic acid has already proven used in a number of settings, including as a cell coating, molecular release mechanism, and producer of nanoparticles. Although the acidic conditions necessary for the assembly of PVA/TA films prevent them from being assembled on living cells, the possibilities for biofunctionalizing PVA allows these films to be fabricated *in vitro* and then targeted to specific cells through after assembly. This allows PVA/TA microcapsules to be used for targeted drug delivery as well as biochemical labeling and sensing. Furthermore, this study deepens the understanding of how polyphenols assemble with polymers in LbL films, allowing for improved fabrication of films based on other polyphenols or small molecules conjugated with polyphenols. With the variety of benefits available from polyphenols, such as their antitumor, antimutagenic, antibacterial, and antioxidant properties, such films could prove valuable for numerous applications.

References

- [1] Decher, G.; Hong, J. D.; Schmitt, J. *Thin Solid Films* **1992**, *210-211*, 831.
- [2] Decher, G. *Science* **1997**, *277*, 1232.
- [3] Hammond, P. T. *Curr. Opin. Colloid In.* **2000**, *4*, 430.
- [4] Schonhoff, M. *Curr. Opin. Colloid In.* **2003**, *8*, 86.
- [5] Bailey, F. E.; Lindberg, R. D.; Callard, R. W. *J. Polym. Sci., Part A* **1964**, *2* (2), 845.
- [6] Ikawa, T.; Abe, K.; Honda, K.; Tsuchida, E. *J. Polym. Sci.* **1975**, *13* (7), 1505.
- [7] Bekturov, E. A.; Bimendina, L. A. *Adv. Polym. Sci.* **1981**, *41*, 99.
- [8] Stockton, W. B.; Rubner, M. F. *Macromolecules* **1997**, *textit30*, 2717.
- [9] Kharlampieva, E.; Kozlovskaya, V.; Tyutina, J.; Sukhishvili, S. A. *Macromolecules* **2005**, *38*, 10523.
- [10] DeLongchamp, D.; Hammond, P. *Langmuir* **2004**, *20*, 5403.
- [11] Kharlampieva, E.; Sukhishvili, S. A. *J. Macromol. Sci. Pol. R.* **2006**, *46*, 377.
- [12] Kharlampieva, E.; Kozlovskaya, V.; Sukhishvili, S. A. *Adv. Mater.* **2009**, *21*, 3053.
- [13] Yang, S.; Zhang, Y.; Zhang, X.; Xu, J. *Soft Matter* **2007**, *3*, 463.
- [14] Podsiadlo, P.; Kaushik, A. K.; Arruda, E. M.; Waas, A. M.; Shim, B. S.; Xu, J.; Nandivada, H.; Pumphlin, B. G.; Lahann, J.; Ramamoorthy, A.; Kotov, N. A. *Science* **2007**, *318*, 80.
- [15] Huang, S.; Cen, X.; Peng, H.; Guo, S.; Wang, W.; Liu, T. *J. Phys. Chem. B* **2009**, *113*, 15225.
- [16] Lee, H.; Mensire, R.; Cohen, R. E.; Rubner, M. F. *Macromolecules* **2012**, *45*, 347.
- [17] Akagama, M.; Suyama, K. *Eur. J. Biochem.* **2001**, *268*, 1953.

- [18] Kozlovskaya, V.; Kharlampieva, E.; Drachuk, I.; Cheng, D.; Tsukruk, V. V. *Soft Matter* **2010**, *6*, 3596.
- [19] Erel-Unal, I.; Sukhishvili, S. A. *Macromolecules* **2008**, *41*, 3962.
- [20] Erel-Unal, I.; Sukhishvili, S. A. *Macromolecules* **2008**, *41*, 8737.
- [21] Zhou, L.; Chen, M.; Tian, L.; Guan, Y.; Zhang, Y. *ACS Appl. Mater. Interfaces* **2013**, *5*, 3541.
- [22] Chanana, M.; Gliozzi, A.; Diaspro, A.; Chodnevskaja, I.; Huewel, S.; Moskalenko, V.; Ulrichs, K.; Galla, H.J.; Krol, S. *Nano Lett.* **2005**, *5*, 2605.
- [23] Krol, S.; del Guerra, S.; Grupillo, M.; Diaspro, A.; Gliozzi, A.; Marchetti, P. *Nano Lett.* **2006**, *6*, 1933.
- [24] Veerabadran, N. G.; Goli, P. L.; Stewart-Clark, S.; Lvov, Y. M.; Mills, D. K. *Macromol. Biosci.* **2007**, *7*, 877.
- [25] Shchepelina, O.; Kozlovskaya, V.; Singamaneni, S.; Kharlampieva, E.; Tsukruk, V. V. *J. Mater. Chem.* **2010**, *20*, 6587.
- [26] De Koker, S.; De Geest, G.; Cuvelier, C.; Ferdinande, L.; Deckers, W.; Hennick, W. E.; De Smedt, S.; Mertens, N. *Adv. Funct. Mater.* **2007**, *17*, 3754.
- [27] Stedler, B.; Chandrawati, R.; Price, A. D.; Chong, S. F.; Breheney, K.; Postma, A.; Connal, L. A.; Zelikin, N.; Caruso, F. *Angew. Chem. Int. Ed.* **2009**, *48*, 4359.
- [28] Kozlovskaya, V.; Harbaugh, S.; Drachuk, I.; Shchepelina, O.; Kelley-Loughnane, N.; Stone, M.; Tsukruk, V. V. *Soft Matter* **2011**, *7*, 2364.
- [29] Mendelson, J. D.; Barrett, C. J.; Chan, V. V.; Pal, A. J.; Mayes, A. M.; Rubner, M. F. *Langmuir* **2000**, *16*, 5017.
- [30] Zhai, L.; Nolte, A. J.; Cohen, R. E.; Rubner, M. F. *Macromolecules* **2004**, *37*, 6113.

- [31] Sukhishvili, S. A.; Granik, S. *Macromolecules* **2002**, *35*, 301.
- [32] Dubas, S. T.; Schlenoff, J. B. *Macromolecules* **2001**, *34*, 3736.
- [33] Shutava, T.; Prouty, M.; Kommireddy, D.; Lvov, Y. *Macromolecules* **2005**, *38*, 2850.
- [34] Matuschek, E.; Svanberg, U. *J. Food Sci.* **2002**, *67*, 420.
- [35] Brune, M.; Rossander, L.; Hallberg, L. *Eur. J. Clin. Nutr.* **1989**, *43*, 547.
- [36] Brune, M.; Hallberg, L.; Skanberg, A. B. *J. Food Sci.* **1991**, *56*, 128
- [37] Chen, H. M.; Hsin, C. F.; Lee, J. F.; Jang, L. Y. *J. Phys. Chem.* **2007**, *111*, 5909.
- [38] Cumberland, S. L.; Strouse, G. F. *Langmuir* **2002**, *18*, 269.